Magnetohydrodynamic Nonlinear Radiative Heat and Mass Transfer Flow of Sisko nanofluid through a Nonlinear Stretching Sheet in The Presence of Chemical Reaction

Abstract: This study considers the problem of the heat and mass transfer of Sisko nanofluids over a nonlinear stretching sheet with magnetohydrodynamics and other physical effects. The model, among other considerations, incorporates the impacts of thermophoresis, Brownian motion, and Biot number in formulating the problem. The flow regime was demonstrated in the form of partial differential equations (PDEs). Through appropriate transformation functions, the PDEs that describe the flow regime are reduced to a set of nonlinear ordinary differential equations. The set of nonlinear ordinary differential equations was treated with Runge-Kutta-Fehlberg's fourth order along with the shooting method. The computational procedure was implemented using the boundary value solver in MAPLE. A detailed analysis is conducted to interpret concisely how the various physical parameters influence velocity, concentration, and temperature. Further, the local Sherwood number and the local Nusselt number are calculated and presented in tabular form. The results were vividly examined graphically and described using the physical variables of interest. The velocity field increased as the Sisko nanofluid material parameter increased. In addition, increasing the reaction parameter decreases the fluid's concentration, whereas a decrease in the reaction parameter favors an increase in the fluid's concentration. The results are presented in detail.

Keywords. Magnetohydrodynamics**,** Nonlinear Sheet, Chemical reaction, Sisko nanofliud, Heat and mass transfer

1. Introduction

Sisko nanofluid is a specific kind of nanofluid that displays shear-thinning behavior, whose viscosity decreases as the shear rate rises. Excellent heat transmission capabilities of Sisko nanofluid have been demonstrated, making it appropriate for use in cooling systems, heat exchangers, and electronic devices, among other applications. [1]. The unique characteristic of Sisko nanofluid lies in its rheological behavior. Traditional nanofluids, such as those derived from water or oil, frequently display Newtonian behavior, where the viscosity remains constant with shear rate. Sisko nanofluid, on the other hand, differs from this pattern of behavior and demonstrates shear-thinning characteristics. This indicates that when the shear rate rises, the viscosity of the substance falls, improving the flow and heat transfer properties [2]. The existence of surface-modified nanoparticles and their interactions with the base fluid are attributed for the Sisko nanofluid's shear-thinning characteristic. Reduced viscosity is the result of the fluid's network-like structure, which the nanoparticles create, disintegrating under shear stress. As a result, the efficiency of heat transmission is increased [3]. This behavior makes it easier to pump through and flow via small channels. The temperature and flow properties of the Sisko nanofluid have been studied in many investigations. According to research studies, Sisko nanofluids, compared to

conventional fluids, can greatly increase the heat transmission coefficient. They have also been discovered to have better thermal conductivity, which improves the efficiency of their heat transfer. [4]. Khan and Shahzad [5] obtained analytical solution to only integral values of the power-law index for the boundary layer equations of a Sisko fluid through a flat stretched. Malik et al. [6] investigated the partial slip effects on the flow and heat transfer of an incompressible Sisko fluid over a nonlinear stretching sheet and stretching cylinder with variable thermal conductivity.

Several industrial and technical operations in the fields of metallurgy and chemical engineering are affected by heat transport phenomena in a laminar boundary layer flow across a stretching sheet. Numerous researchers have examined the flow past a stretching surface with various stretching velocities, including linear, exponential, quadratic, hyperbolic, radially, and even oscillatory. [7, 8, 9]. However, there are only a few studies on the transfer of heat and mass in laminar boundary layer flow through a nonlinear stretching sheet. It is widely known in literature that stretching in many industrial applications is not always linear, for this reason academics have studied nonlinear stretching sheets for various fluid flows. Rashidi et al. [10] conducted a lie group analysis to examined freeconvective flow of a nanofluid through a horizontal porous plate in the presence of chemical reaction. The mixed convective heat and mass transport of nanofluids over a nonlinear stretching sheet under the influence of suction/injection parameter, magnetic parameter, and thermophoresis parameter has been studied by Mondal et al. [11] in their analysis. The shooting technique was used by Dhanai et al. [12] to investigate the impact of viscous dissipation for the problem of magneto-hydrodynamic boundary layer flow of nanofluid that results from a power-law stretching/shrinking permeable sheet. The problem of boundary layer flow of nanofluid through nonlinear permeable stretching sheet at specified surface temperature in the presence of partial slip has been investigated numerically by Das [13]. Megahed et al. [14] have researched on the significance of thermal buoyancy and continuous heat flux on the steady two-dimensional flow and heat transfer of non-Newtonian power-law fluid under the influence of thermal radiation.The two-dimensional boundary layer flow of a viscous, incompressible, and electrically conducting fluid over a nonlinearly stretching non-isothermal sheet in the presence of a variable transverse magnetic field, thermal radiation, viscous dissipation, and a nonlinearly moving free stream was studied numerically by Kumbhakar and Rao [15]. The motion of MHD heat and mass transfer of nanofluid due to a stretching sheet through a porous medium with radiation effect was implemented by Reddy et al. [16]Many technical processes, such as nuclear power plants, gas turbines, and the numerous propulsion systems for airplanes, missiles, satellites, and spacecraft, use heat transfer, which is influenced by thermal radiation. It is important to note that the nonlinear approximation problem is controlled by three parameters, including the Prandtl number, radiation parameter, and temperature

ratio parameter, whereas the linearized Rosseland approximation only uses the effective Prandtl number as a dimensionless parameter. Krishnamurthy et al. [17] considered the magnetohydrodynamic and nonlinear radiative heat transfer of sisko nanofluid through a nonlinear stretching sheet under the influence of chemical reaction. The problem of Sisko liquid over a stretching surface in the presence of nonlinear thermal radiation, chemical reaction and magnetic field has been perused by Nagendramma [18]. A flat plate with partial slip at the surface subjected to the convective heat flux in the presence of nonlinear thermal radiation was explored by Parida et al. [19] for two-dimensional steady MHD boundary layer flow of heat and mass transfer. The boundary layer flow induced by a continuous stretched sheet in a quiet fluid in the presence of nonlinear Rosseland thermal radiation was the subject of a computational approach carried out by Cortell [20]. Using a novel radiation parameter known as the film radiation parameter, Pantokratoras [21] examined the impact of linear and nonlinear Rosseland radiation on steady laminar natural convection down a vertical isothermal plate.

Equally, non-Newtonian nanofluids have gained prominence during the past year because of their industrial applications. It has been demonstrated previously that the use of a working fluid containing nanoparticles may significantly improve the efficiency and performance of heat transfer phenomena. Numerous studies have placed emphasis on non-Newtonian fluid over a stretched sheet as the basic fluid with dispersed nanoparticles. For instance, the effects of thermophoresis and Brownian motion on the flow of Jeffrey nanofluid in a three-dimensional boundary layer and convective heat transfer through a bidirectional stretching surface were investigated by Hayat et al. [22] utilizing a recently developed boundary condition with zero nanoparticle mass flux. In the presence of thermal radiation, Brownian motion, and thermophoresis effects, Khan et al.[23]have implemented the impact of convective boundary conditions on two-dimensional boundary layer flow and heat transfer of Sisko nanofluid over a nonlinearly stretching sheet.Mabood et al. [24] have researched the consequences ofnon-uniform heat sources on steady two-dimensional hydromagnetic mixed convective heat and mass transfer flow of a micropolar fluid over a stretching sheet embedded in a non-Darcian porous medium with thermal radiation, variable thermal conductivity, Soret parameter andviscous-Ohmic dissipation.Heat and mass transfer of two-phase nanofluid flow in a rotating system in the presence of a transverse magnetic field have been addressed analytically by Ebiwareme et al. [25] using an Adomian decomposition approach. It was found in their study, that the pertinent parameters have profound influence on the flow distributions. Masood et al. [26] studied the flow of heat transfer on Sisko nanofluid across a nonlinear stretching sheet. The influence of thermal radiation on the convective heat and mass transfer flow of a Sisko

nanofluid across a nonlinear stretching sheet has been taken into consideration by Venkata et al. [27]

In view of the above, the motivation of this present study is to examine the nonlinear radiative flow of magnetohydrodynamic Sisk nanofluid over an exponentially stretching sheet in the presence of a chemical reaction and a concentration-based internal heat source. Through appropriate similarity transformations for velocity, temperature, and concentration, the governing equations for flow, heat, and mass transfer were transformed into a set of ordinary differential equations. The emerging equations subjected to the boundary conditions were solved numerically using the convectional Runge-Kutta-Fehlberg and shooting techniques. The numerical investigation is performed for various thermo physical parameters such as the heat parameter, Prandtl number, nano Lewis number, Brownian motion parameter, radiation parameter, thermophoresis parameter, and chemical reaction parameter. The results obtained, which reflect excellent agreement with established literature, are validated through comparison. The study is categorized as follows. In section one, introduction of the study exploring exhaustive literatures for possible gaps in the study is given. The mathematical formulation comprising the governing equation as well as the reduction of the governing boundary layer equations subject to the prescribed boundary conditions using self-similar transformation is presented in section two. In the next section, solution to the nondimensionalised equation for the flow distributions including Nusselt and Sherwood numbers are implemented using MAPLE Solver. Section four gives the presentation of the results for different values of the pertinent parameters presented in graphs and figures. The conclusion of the study highlighting the major outcomes is given in section five.

2. Mathematical Formulations

We examine a laminar, two-dimensional, continuous flow of a Sisko nanofluid in the domain $y > 0$, induced by a stretching sheet with a power-law velocity profile,$U = cx^s$. Here, c denotes a non-negative real constant and $s > 0$ represents the rate at which the sheet is stretched. The temperature of the stretched surface and nanoparticles are considered to be constant variables, represented by T_w andC_w, respectively. When y tends to infinity, the ambient values of temperature and nanoparticle fraction are denoted by T_∞ and C_∞, respectively. The magnetic field is applied normally to the stretching sheet. The flow is along the x-axis, while the y-axis is normal to the plane of the sheet, as shown in figure 1 below. Essentially, the fixed temperature and nanoparticle fraction for the stretching surface are presumed greater than the ambient temperature and nanoparticle fraction.

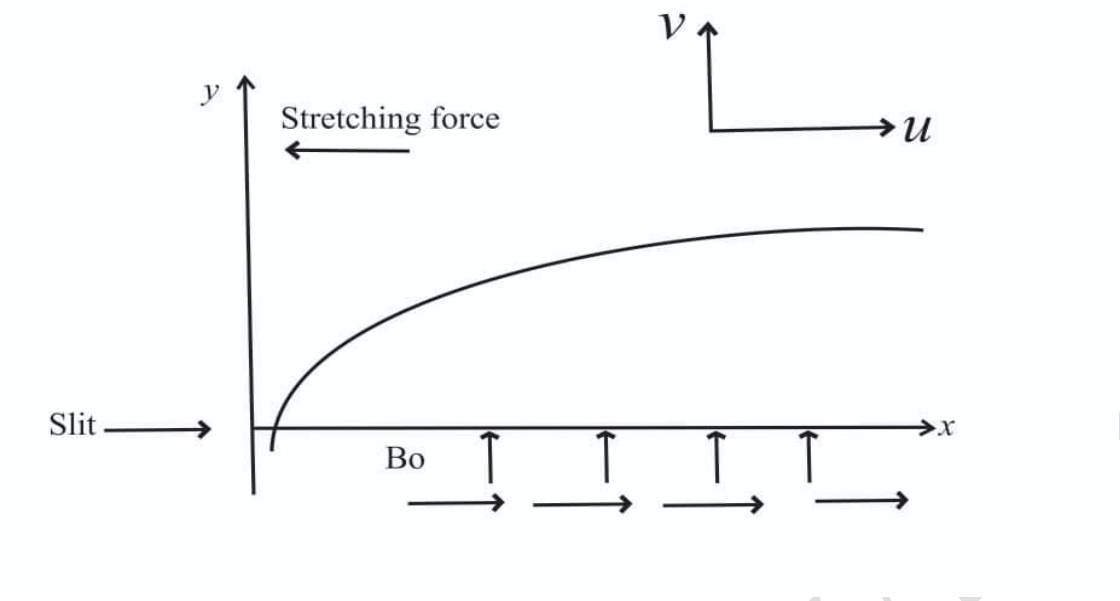

Figure 1.Physical configuration of the model

In the context of the assumptions stated herein, the appropriate equations (Venkatta et al, 2016)

$$\frac{\partial u}{\partial x}+\frac{\partial v}{\partial y}=0 \quad (1)$$

$$u\frac{\partial u}{\partial x}+v\frac{\partial u}{\partial y}=\frac{\alpha}{\rho}\frac{\partial^2 u}{\partial y^2}-\frac{b}{\rho}\frac{\partial}{\partial y}\left(-\frac{\partial u}{\partial y}\right)^r-\frac{\sigma B_0^2}{\rho}u \quad (2)$$

$$u\frac{\partial T}{\partial x}+v\frac{\partial T}{\partial y}=\frac{\partial}{\partial y}\left(\alpha+\frac{16\sigma^* T_\infty^3}{3\rho C_P k^*}\right)\frac{\partial T}{\partial y}+\tau\left[D_B\frac{\partial C}{\partial y}\frac{\partial T}{\partial y}+\frac{D_T}{T_\infty}\left(\frac{\partial T}{\partial y}\right)^2\right] \quad (3)$$

$$u\frac{\partial C}{\partial x}+v\frac{\partial C}{\partial y}=D_B\frac{\partial^2 C}{\partial y^2}+\frac{D_T}{T_\infty}\frac{\partial^2 T}{\partial y^2}-k_1(C_w-C_\infty) \quad (4)$$

The associated boundary conditions prescribed in this problem are given as

$$u(x,y)=U=cx^s, v(x,y)=0, k\frac{\partial T(x,y)}{\partial y}=-h_f\left(T_f-T(x,y)\right)\text{at } y=0$$

$$D_B\frac{\partial C(x,y)}{\partial y}=-k_m\left(C_f-C(x,y)\right) \quad (5)$$

$u\longrightarrow 0, T\longrightarrow T_w, C\longrightarrow C_\infty$ as $y\longrightarrow\infty$

Let u and v denote the velocity components along the x and y axes, respectively. The material constants of the Sisko fluid are represented by a, b, and r ($r\geq 0$), T refers to the temperature of the fluid, C is the mass concentration of the solid nanoparticle volume fraction, $\rho, \sigma, \alpha, andk$ are the fluid density, electrical conductivity, thermal diffusivity, and thermal conductivity, $D_B$denotes the Brownian motion diffusion coefficient and$D_T$represent the thermophoresis coefficient.

The non dimensionless velocity, temperature and the nanoparticles fraction volume are defined as follows.

$$f' = \frac{u}{U}, \theta = \frac{T-T_\infty}{T_f-T_\infty}, \varphi = \frac{C-C_\infty}{C_f-C_\infty} \quad (6)$$

where$T - T_\infty$, $T_f - T_\infty, C - C_\infty$, $C_f - C_\infty$ are the fluid temperature, and the concentration of Sisko nanoparticles respectively.Following Venkatta et al. (2016), we define the similarity transformationgroup given by

$$\eta = \frac{y}{x} Re_b^{\frac{1}{r+1}}, v(x,y) = -URe_b^{\frac{1}{r+1}} \frac{1}{r+1} [\{s(2r-1)+1\} f(\eta) + \{s(2-r)-1\} \eta f'(\eta)],$$

$$u(x,y) = Uf'(\eta) \quad (7)$$

The non dimensional variables are.

$$Re_a = \frac{\rho x U}{a}, Re_b = \frac{\rho x^r U^{2-r}}{b}, \text{A}=\frac{Re_b^{\frac{2}{r+1}}}{Re_a}, P = \frac{XU}{\alpha} Re_b^{\frac{2}{r+1}}, \ B_{i_1} = \frac{h_f}{k} xRe_b B = \frac{\tau D_B (C_f - C_\infty)}{\alpha}, \quad T_p =$$

$$\frac{\tau D_T (T_f - T_\infty)}{T_\infty \alpha}, \ Le = \frac{\alpha}{D_B}, B_{i_2} = \frac{h_m}{k} xRe_b^{\frac{-1}{r+1}}, \ \text{R} = \frac{16\sigma \text{T}_\infty^3}{3\text{k}\rho\text{C}_\text{p}}, k_1 = \frac{\gamma a}{Le} D_B = \frac{\propto}{Le} M = \frac{Re_a \sigma B_0^2}{Re_b^{\frac{1}{r+1}}}, \gamma = \frac{k_1 Le}{a} \quad (8)$$

Using Eqs (6), (7) and (8), the governing Eqs. (1−4) reduced to the form.

$$Af''' + r(-f'')^{r-1} f''' + \left(\frac{s(2r-1)+1}{r+1}\right) ff'' - sf'^2 - Mf' \quad (9)$$

$$\left(\frac{1}{1+R}\right) \theta'' + P \left(\frac{s(2r-1)+1}{r+1}\right) f\theta' + B\varphi'\theta' + T_p \theta'^2 = 0 \quad (10)$$

$$\varphi'' + Le \left(\frac{s(2r-1)+1}{r+1}\right) f\varphi' + \frac{T_p}{B} \theta'' - \gamma\varphi = 0 \quad (11)$$

The corresponding transformed boundary conditions are given asfollows.

$$f(0) = 0, f'(0) = 1, \theta'(0) = -B_{i_1}[1 - \theta(0)], \varphi(0) = 1$$

$$f' \to 0, \theta \to 0, \varphi \to 0 \ as \ \eta \to \infty \quad (12)$$

In the above equations, primes represent differentiation with respect to $\eta, \gamma = \frac{k_1 Le}{a}$is the chemical reaction parameter, $M = \frac{Re_a \sigma B_0^2}{Re_b^{\frac{1}{r+1}}}$ for magnetic parameter, $R = \frac{16\sigma \text{T}_\infty^3}{3\text{k}\rho\text{C}_\text{p}}$ for radiation parameter, $Le = \frac{\alpha}{D_B}$ Lewis number, $B = \frac{\tau D_B (C_f - C_\infty)}{\alpha}$is the Brownian motion parameter,$T_p = \frac{\tau D_T (T_f - T_\infty)}{T_\infty \alpha}$is the thermophoresis parameter, $P = \frac{XU}{\alpha} Re_b^{\frac{2}{r+1}}$ for the generalized Prandtl number, $A = \frac{Re_b^{\frac{2}{r+1}}}{Re_a}$ material parameter of the Sisko fluid, $Re_a = \frac{\rho x U}{a}$, and $Re_b = \frac{\rho x^r U^{2-r}}{b}$ are the local Reynolds numbers, a, b, and r are the material constants of the Sisko fluid, and $B_{i_1} = \frac{h_f}{k} xRe_b$ isthe generalized thermal Biot number,

The physical quantities of interest are the Local skin friction, C_{fx}Nusselt number, N_{ux} and Sherwood number, Sh_x. These are expressed as.

$$C_{fx} = \frac{\tau_w}{\frac{1}{2}\rho U^2}, N_{ux} = \frac{xq_w}{k(T_w - T_\infty)}, Sh_x = \frac{xj_w}{k(C_w - C_\infty)} \quad (13)$$

Here τ_w, q_w, and j_w are the shear stress along the stretching surface, heat flux, and the surface mass flux respectively whose expressions are stated below as

$$\tau_w = \left(a + b\left|\frac{\partial u}{\partial y}\right|^{r-1}\right)\frac{\partial u}{\partial y} \qquad \text{at } y = 0$$

$$q_w = -k\frac{\partial T}{\partial y} + (q_r)_w \text{ at } y = 0 \quad (14)$$

$$j_w = -D_B\frac{\partial C}{\partial Y}\text{at} \qquad \text{y s= 0s}$$

Plugging Eqs. (6) and (7) in (13) we have the non-dimensional forms as

$$\frac{1}{2}Re_b^{\frac{1}{r+1}}C_{fx} = Af''(0) - [f''(0)]^r \quad (15)$$

$$Re_b^{-\frac{1}{r+1}}N_{ux} = -\theta'(0) \quad (16)$$

$$Re_b^{-\frac{1}{r+1}}Sh_x = -\varphi'(0) \quad (17)$$

3.Method of solution

The Runge-Kutta-Fehlberg fourth-order methodcombined with the shooting method is used to solve the set of nonlinear boundary value problems sin Eqs. (9)– (11) subject to the boundary conditions (12) (Malik et al, 2014 Munir et al 2014). Using transformational variables, Eqs. (9), (10), and (11)subject to Eq. (12) are discretized into a system of first-order ODEs in Eqs. (19), (21), and (23) with condition (24).

$$f = y_1, f' = y_2, f'' = y_3, f''' = yy_1 \quad (18)$$

$$yy_1 = \frac{-1}{A + r(y_3)^{r-1}}\left[\left(\frac{2(2r-)+1}{r+1}\right)y_1y_3 - sy_2^2 - My_2\right] \quad (19)$$

$$\theta = y_4, \theta' = y_5, \theta'' = yy_2 \quad (20)$$

$$yy_2 = \frac{-1}{1+R}\left[P\left(\frac{2(r-1)+1}{r+1}\right)y_1y_5 + By_7y_5 + T_py_5^2\right] \quad (21)$$

$$\varphi = y_6, \ \varphi' = y_{7,}\varphi'' = yy_3 \quad (22)$$

$$yy_3 = -L_e\left(\frac{2(r-1)+1}{r+1}\right)y_1y_7 - \frac{T_P}{B}yy_2 + \gamma y_6 \quad (23)$$

The associated boundary conditions are.

$$y_1(0), y_2(0) - 1, y_5(0) + B_{i_1}[1 - y_4(0)], y_2 \to 0, y_4 \to 0, y_6 \to 0 \ as \ \eta \to \infty \quad (24)$$

The set of discretized Eqs. (19), (21), and (23) with boundary condition, Eq. (24), is solved numerically using a shooting algorithm with a Runge-Kutta Feldberg integration scheme. This method involves transforming the problem into initial values that must be determined through guessing, and a fourth order Runge – Kutta iteration scheme is employed to integrate the set of initial value problems until the given boundary conditions are satisfied. The computational procedure was implemented using the Maple solver.

4.Results and Discussions

This section discusses the main properties of the physical parameters presented in Eqs. (9) through (11). These include the thermophoresis parameter, generalized Prandtl number, Lewis number, Brownian motion parameter, magnetic parameter, and temperature-dependent Biot number, among others.

Table 1 depicts a comparative analysis of the reduced Nusselt number compared to the results declared and published by [26, 5, 17, & 27]. The values have been compared with various values of P for 0.7, 0.2, 7.0, and 20.0, respectively. The table revealed that the present results agree well with the earlier published works as cited.

For different values of the magnetic field parameter, the velocity field is plotted against the similarity variable in Figs. 2 and 3. The figures show that, for both linear and nonlinear stretching sheets, the velocity decreases as the magnetic field parameter (i.e., the ratio of electromagnetic force to viscous force) increases. The impact of the magnetic field parameter M on the fluid temperature and concentration is shown in Figs. 4, 5, 6, and 7. As depicted in the profiles, increasing magnetic field strength favors an increase in fluid temperature and concentration. This is because of the Lorentz force, which is a resistive force created when a magnetic field is introduced to an electrically conducting fluid. The velocity of the boundary layer fluid was reduced by this force. The magnetic field, M, is observed as thermal energy in addition to the additional work required to drag the conducting nanofluid against the action of the magnetic field. In the presence of

a magnetic field, the thickness of the thermal boundary layer increases, whereas the thickness of the momentum boundary layer decreases.

For nonlinear stretching sheets with r = 2, Fig. 8 shows the effect of changing the generalized Prandtl number P on the dimensionless temperature. The temperature profile and related boundary thickness decreases as the Prandtl number increases. The thermal diffusivity weakens when the Prandtl number P continues to increase. Larger Prandtl numbers have poorer thermal diffusivity from a physical standpoint, while smaller Prandtl numbers have better thermal diffusivity. The temperature and thermal boundary layer are reduced owing to the gradient between the effects of high and low Prandtl numbers on thermal diffusivity. The effect of various Le values on the concentration profile of the nonlinear stretching sheet is shown in Fig. 9. Recall that, in the boundary layer phase,Le quantifies the ratio of the thermal diffusion rate to species diffusion rate. The figures demonstrate that when Le increases, the thermal boundary layer thickness decreases and were accompanied by a decrease in temperature and mass transfer. Further, this shows how increasing Le affects the concentration distribution significantly. As Le increases, the volume fraction boundary layer decreases across the plate. Figs. 10 and 11 show the effect of various values of the thermophoresis parameter T_p on the dimensionless temperature and concentration, while Figs. 12 and 13 show the impact of Brownian motion parameters for r = 2 on the dimensionless temperature and concentration. The graphs show that for the nonlinear stretching sheet, a reduction in the Brownian motion parameter decreases the temperature profile while increasing the concentration profile. However, both the temperature and concentration profiles decrease when the thermophoresis parameter is decreased. Figs.13 and 14 shows the effect of decreasing the Biot number on the concentration of the Sisko nanofluid. The concentration of the fluid decreases as the Biot number decreases.

Furthermore, Figs. 15 and 16 illustrate how various chemical reaction parameter values for species consumption and generation instances affect the dimensionless concentration for r = 2. In the given

situations, it is observed that the concentration decreases for the constructive chemical reaction parameter and increases for the destructive chemical reaction parameter. This is because the molecule is consumed during systemic chemical processes, which lowers its concentration profile. The primary result is that the overshot in the profiles of solute concentration in the solute boundary layer can be reduced by a first-order chemical reaction. The impact of various Sisko nanofluid material parameter values, *A*, on the dimensionless velocity profile is shown in Fig. 17. Recall that the consistency index and high shear rate viscosity are represented by the material parameter *A*. The graph clearly shows that the velocity distribution increases as the Sisko nanofluid material parameter, *A*, increases. This is because an increase in *A* reduces the consistency index (i.e., viscosity) of the fluid, which increases the fluid's velocity. Figure 18 shows the effect of thermal radiation on the temperature profile of the nonlinear sheet ($r = 2$). It is evident from the profiles that the temperature distribution increases as *R* decreases. This suggests that lowering the thermal radiation parameter increased the boundary layer thickness of the fluid.

The impacts of the nonlinear stretching parameter (r) on the temperature and velocity distributions are shown in Figs. 19 and 20, respectively. Clearly, as r increases, the temperature profile of the nanofluid also increases rapidly, whereas the velocity profile is only marginally affected.

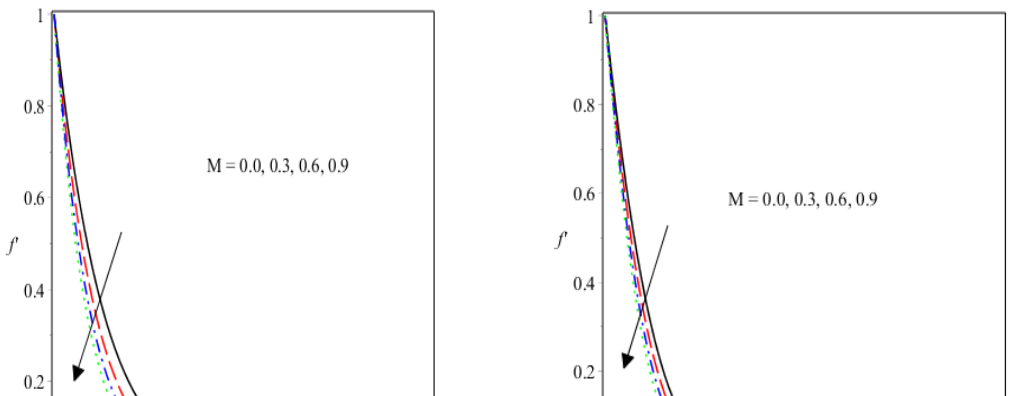

Fig. 2 Effect of Mon velocity($r = 1$)

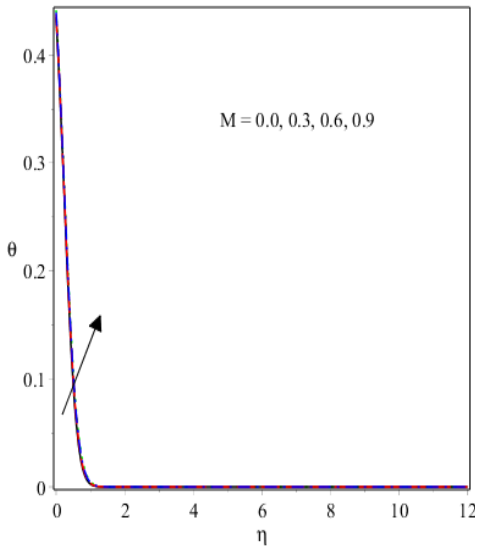

Fig. 3 Effect of M velocity profile($r = 2$)

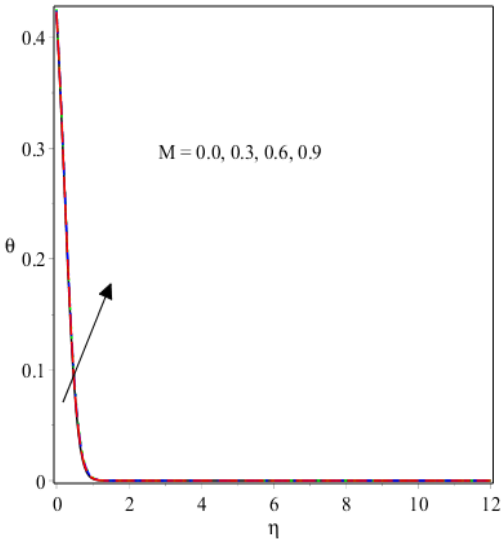

Fig. 4 Effects of M on temperature($r = 1$)

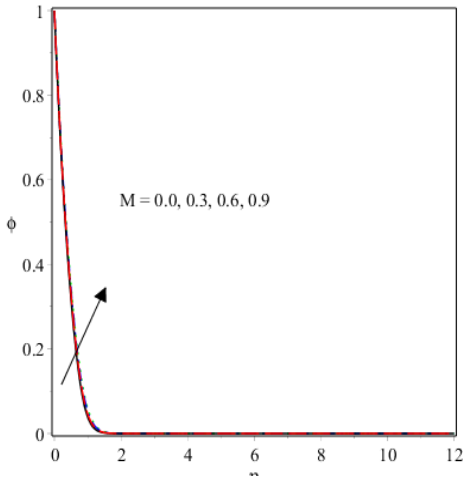

Fig. 5 Effects of M temperature($r = 2$)

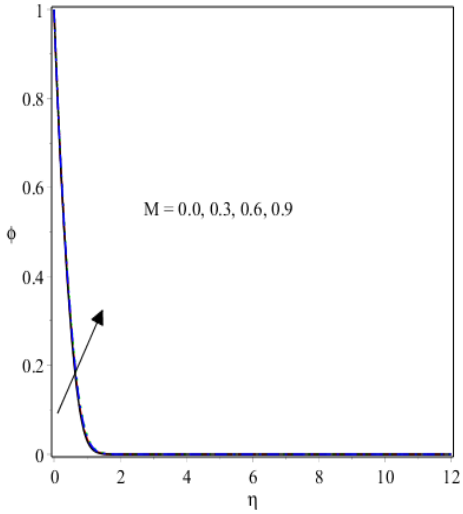

Fig. 6 Effects of M on concentration (r= 1)

Fig. 7 Effects of Mconcentration ($r = 2$)

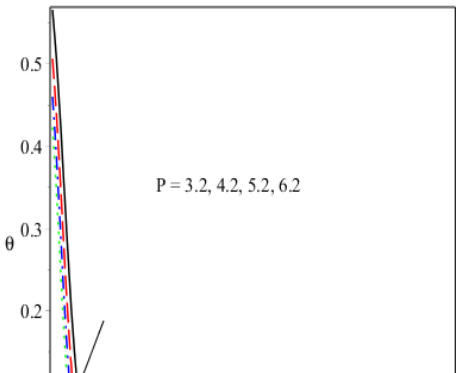

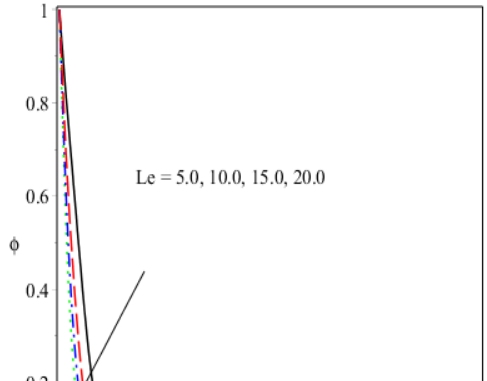

Fig. 8 Effect of P on temperature $(r = 2)$

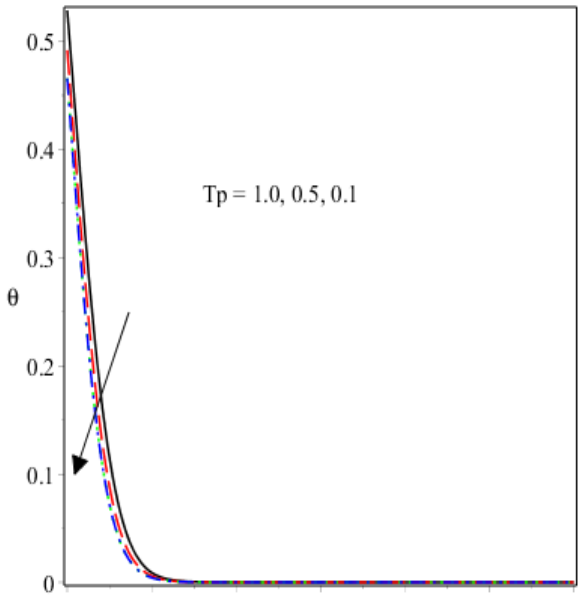

Fig.9 Effect of varying Le concentration $(r = 2)$

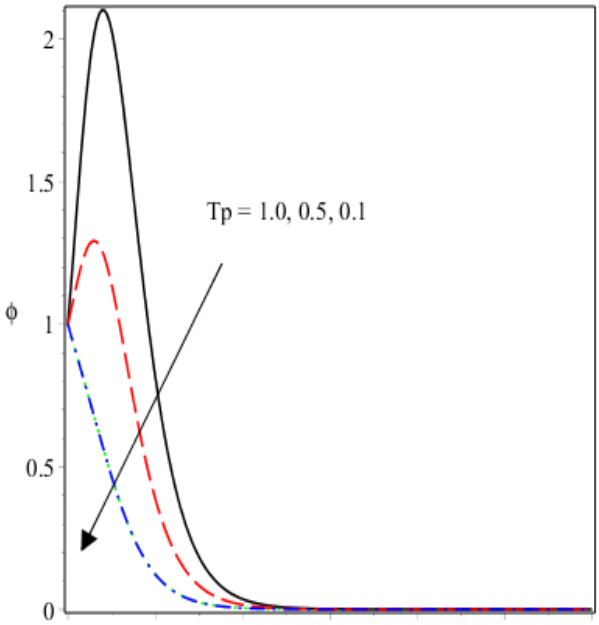

Fig. 10 Effect ofvarying temperature$(r = 2)$

Fig. 11 Effect of varying T concentration $(r = 2)$

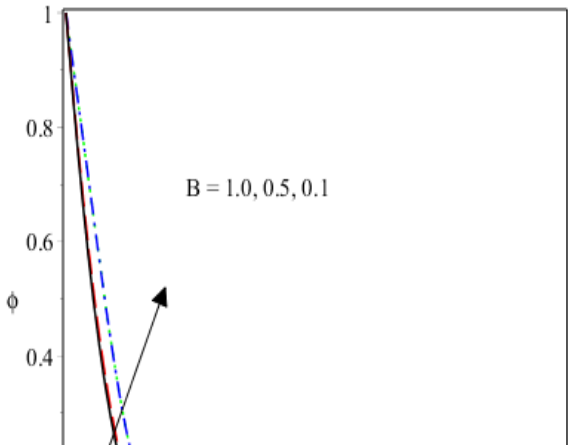

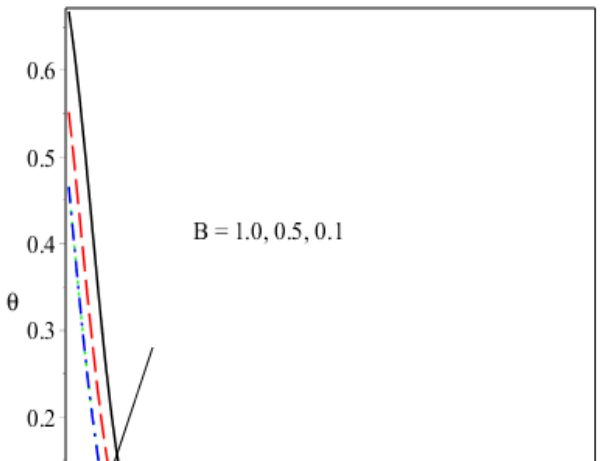

Fig. 12 Effect of B on concentration($r = 2$)

Fig 13 Effect of B temperature ($r = 2$)

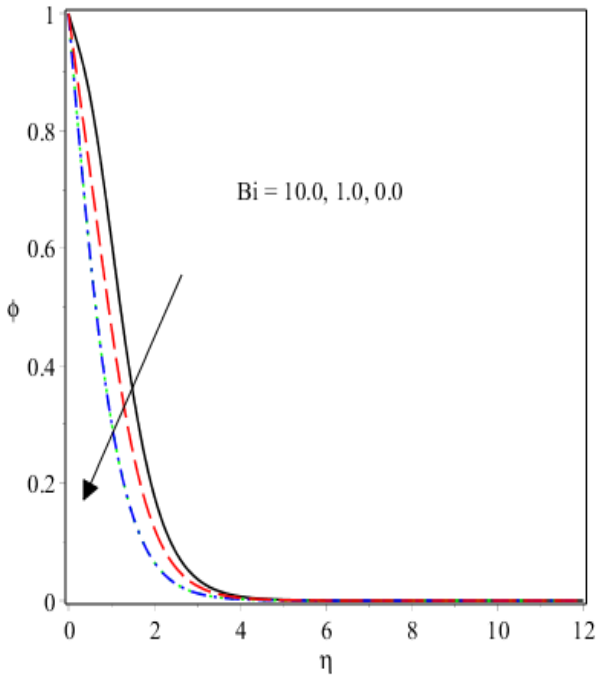

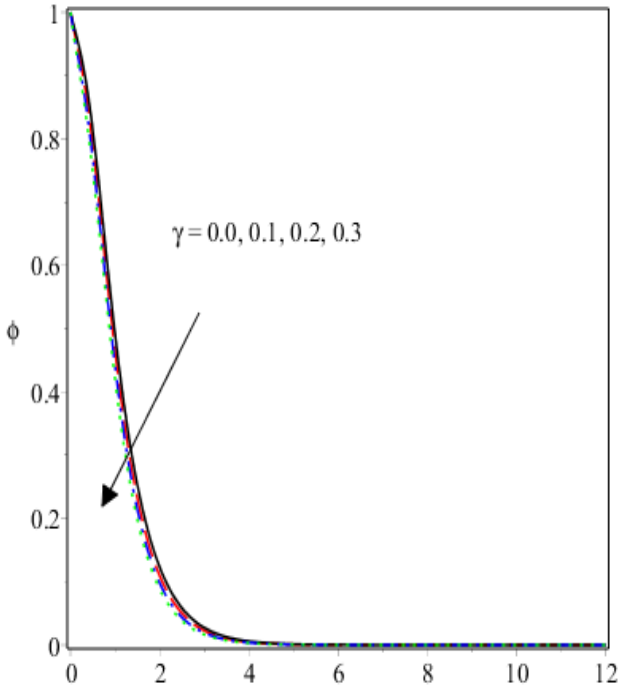

Fig. 14 Effect of Bion concentration($r = 2$)Fig.15 Effect of γ, on concentration ($r = 2, Le = 2.0$)

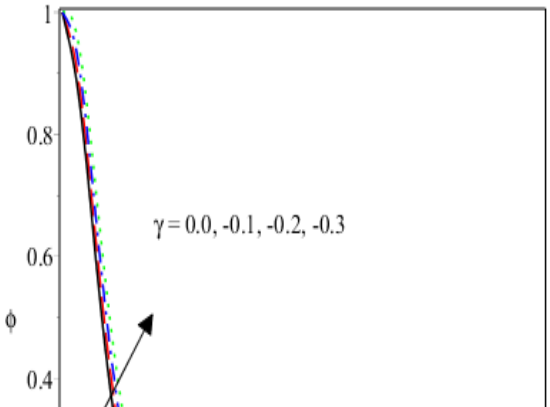

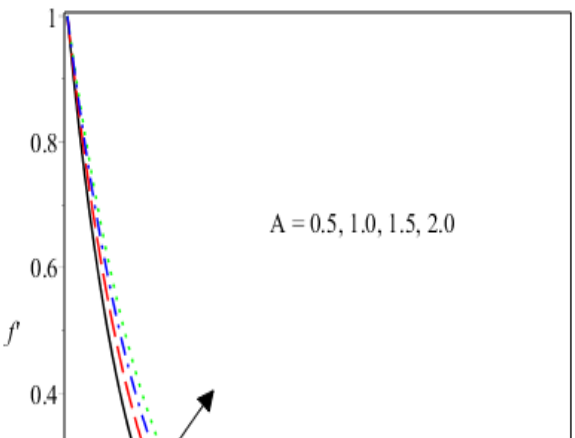

Fig. 16 Effect of chemicalreactionγ, on concentration (r = 2, Le =2.0)

Fig. 16 Effect of γ on concentration $(r = 2, Le = 2)$

Fig. 17 Impact of Aon velocity profile

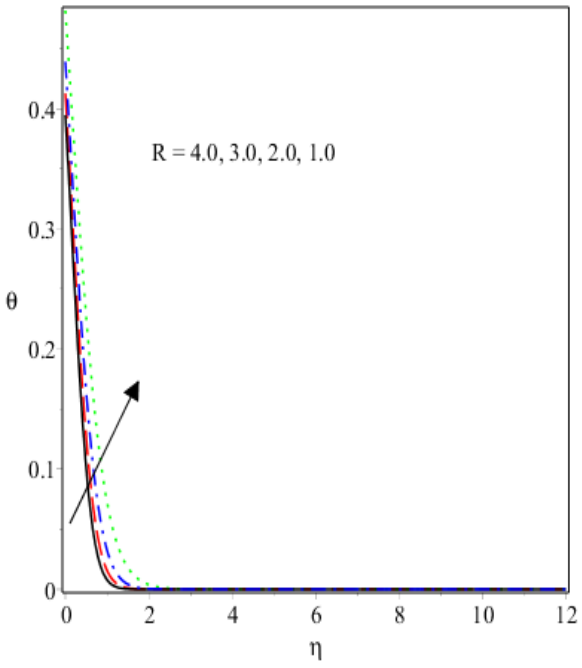

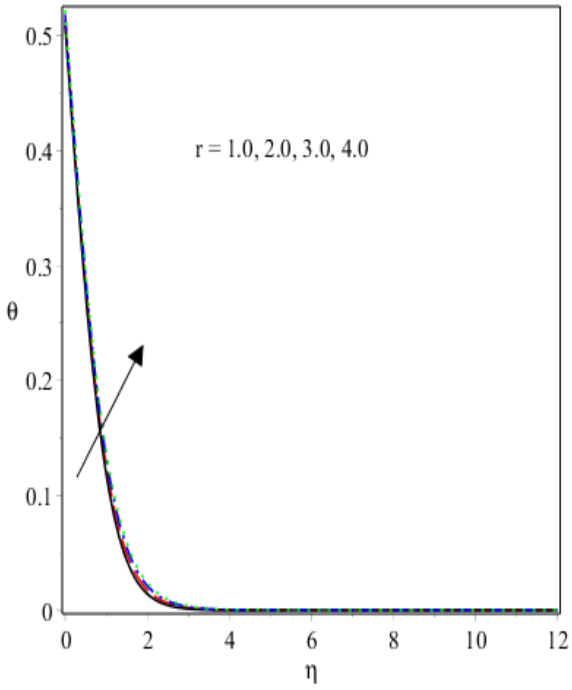

Fig. 18 Influence of R temperature $(r = 2)$

Fig. 19 Influence of r on temperature

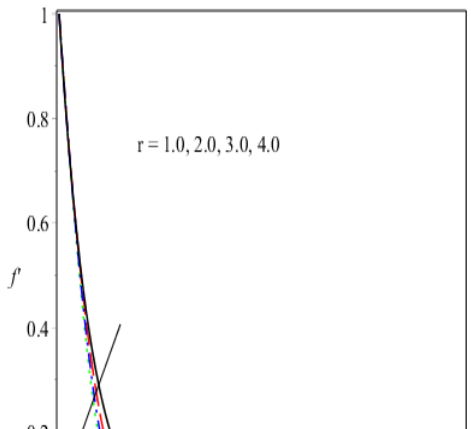

S

Fig. 20 Influence of$r$ on velocity profile

Table 1 Comparison of results for reduced Nusselt number $-\theta'(0)$ for $A= B =M=R=B_{i1}=S=0$

P	Masood [26]	Khan& Shahzad [5]	Prasanna kumara et.al [17]	Venkatta et.al [27]	Present results
0.7	0.4539	0.4539	0.4544	0.454470	0.36234
2.0	0.9113	0.9113	0.9113	0.911353	0.78345
7.0	1.8954	1.8954	1.8954	1.895400	1.75342
20.0	3.35395	3.3539	3.3539	3.353902	3.37234

5.Concluding Remarks

The effect MHD on the flowof a Sisko nanofluid with mass transfer under a nonlinear stretching sheet was investigated. The effects of the pertinent parameters on the dimensionless velocity, dimensionless temperature, and dimensionless concentration are considered and presented graphically. The following conclusions are drawn from our study.

i. The velocity profile declines in the presence of the parameters$A$ and$M$.

ii. Increasing M and r enhances the temperature profile.

iii. There is enhancement of concentration as a result of increased magnetic field parameters. This is also observed in the case of the destructive chemical reaction parameter, where the concentration is enhanced.

iv. Increase in P lead to a decrease in the temperature profile.

v. The temperature and concentration profiles decrease as the Brownian motion decreases.

vi. A decrease in the Biot number decreases the fluid's concentration while increasing the temperature profile.

vii. Decreasing the thermophoresis parameter favors a decrease in both concentration and temperature profiles.

viii. Increasing *Le* significantly decreased the volume fraction of the boundary layer across the plate.

References

1. Sisko, J.(2010). Shear Thinning Nanofluids. US Patent No. 7,772,012.

2. Sisko, J. Zhang, D. (2012).Experimental investigation of the rheological behavior of shear-thinning nanofluids. Journal of Nanoparticle Research, 14(1), 1-10.

3. Sisko, J, Zhang, D. (2014). Heat transfer and flow characteristics of shear-thinning nanofluids. International Journal of Heat and Mass Transfer, 77, 115-123.

4. Sisko, J,Zhang, D. (2016). A review on the rheological behavior of shear-thinning nanofluids. Journal of Nanofluids, 5(1), 1-17.

5. Khan M, Shahzad, A. (2013). On boundary layer flow of Sisko fluid over stretching sheet. QuaestionesMathematicae, Volume3, (5), 137–51.

6. Malik R, Khan M, Munir A, Khan W,A. (2014). Flow and heat transfer in Sisko fluid withconvective boundary condition. PLOS ONE,9(10), 107989.

7. Nandeppanavar M, M., Vajravelu K, Subhas Abel, M. Chiu-On N (2011). Heat transfer over anonlinearly stretching sheet with non-uniform heat source and variable walltemperature.Int J Heat Mass Transfer, 54, (5), pp. 23–36.

8. Ahmad A, Asghar, S.(2012). Flowand heat transfer over hyperbolic stretching sheets. AppliedMathematicsand computation33(4):445–54.

9. Murshed F, K., Chowdhury I, R (2015). Chattopadhyay A, Sandeep N. Radiation effect on boundary layer flow of a nanofluid over a nonlinearly permeable stretching sheet.Adv Phys Theor Appl, 40, 2225–0638.

10. Rashidi M, M., Momoniat E, Ferdows M, Basiriparsa A. (2014). Lie group solution for freeconvective flow of a nanofluid past a chemically reacting horizontal plate in aporous media. Article ID 239082 Math Problems Eng.

11. Mondal H, Mishra S, Bera U, K. (2015). Nanofluids on MHD mixed convective heat and mass transfer over a nonlinear stretching surface with suction/injection.J Nanofluids,4(2):223–9.

12. Dhanai R, Rana P, Kumar, L. (2015). Multiple solutions of MHD boundary layer flow and heat transfer behavior of nanofluids induced by a power-law stretching/shrinking. Permeable sheet with viscous dissipation. Powder Technol, 273, 62–70.

13. Das, K. (2015). Nanofluid flow over a nonlinear permeable stretching sheet with Partial slip.Journal of Egyptian Mathematical Society, 23, 451–466.

14. Megahed A, M. (2015). Flow and heat transfer of a non-Newtonian power-law fluidover a nonlinearly stretching vertical surface with heat flux and thermal radiation, Mechanica, 50(7), 1693–700.

15. Gnaneswara R, M., Padma P, Shankar B, Gireesha B, J. (2016). Thermal radiation effects onMHDstagnation point flow of nanofluid over a stretching sheet in a porous medium.J Nanofluids, 5(5), 753–64.

16. Magyari E, Pantokratoras A. (2011). Note on the effect of thermal radiation in the linearizedRosseland approximation on the heat transfer characteristics of various boundary layer flows. Int Commun Heat Mass Transfer, 38, 554–656.

17. Prasannakumara, B, C.,Gireesha, B, J., Krishnamurthy, M, R. (2017). Ganesh Kumar, K. MHD flow and nonlinear radiative heat transfer of Sisko nanofluid over a nonlinear stretching sheet. Informatics in Medicine Unlocked, 9, 123-132.

18. Nagendramma, V. (2020). Magnetohydrodynamic chemically reactive Sisko liquid flow through a stretching surface with nonlinear thermal radiation., Journal of Physics Conference Series, 15597, 012037.

19. Parida S, K., Panda S, Rout, B,R.(2015). MHD boundary layer slip flow and radiative nonlinearheattransfer over a flat plate with variable fluid properties and thermophoresis.Alexandria Eng J, 54(4), 941–953.

20. Cortell,R.(2014). Fluid flow and radiative nonlinear heat transfer over a stretching sheet. J King Saud Univ – Sci, 26, 161–177.

21. Pantokratoras, A. (2014). Natural convection along a vertical isothermal plate with linear and nonlinear Rosseland thermal radiation. Int J Therm Sci, 84, 151–165.

22. Hayat T, Muhammad T, Shehzad S, A., Alsaedi A. (2015). Three-dimensional flow of Jeffrey nanofluid with a new mass flux condition.Aerospace Engineering,1061/(ASCE)AS.1943-5525.0000549J, 04015054.

23. Khan M, Malik R, Munir A, Khan W, A. (2015). Flow and heat transfer to Sisko nanofluid overa nonlinear stretching sheet. PLOS ONE 2015;10(5):0125683. http://dx.doi.org/10.1371/journal.pone.0125683.

24. Mabood F, Ibrahim S, M, Rashidi M, M.,Shadloo M, S., Lorenzini, G. (2016). Non-uniform heat source/sink and Soret effects on MHD non-Darcian convective flow past a stretching sheet in a micropolar fluid with radiation.Int J Heat Mass Transfer, 93, 674–82.

25. Ebiwareme, L, Bunonyo, K, W., Davies, O, A. (2023). Analytical solution for heat and mass transfer of two-phase nanofluid flow with magnetic field in a rotating system using Adomian decomposition method.International Journal of Scientific and innovative mathematical research, Volume 11, Issue 2, pp. 1-16.

26. Masood, K, Rabia, M., Munir, Waqar Azeem, K. (2015). Flow and Heat transfer of Sisko nanofluid over a nonlinear stretching sheet.PLOS ONE.

27. Venkatta R, G., Sreedhar B, M.,Lavanaya, M. (2016). Convective heat and mass transfer flow of Sisko nanofluid past a nonlinear stretching with thermal radiation. International Refereed Journal of Engineering and Science, Volume 5, Issue 2, pp. 17-37.

28. Malik, R,Khan, M, Munir, A, Khan W, A. (2014). Flow and Heat Transfer of Sisko Fluidwith convective Boundary Condition (2014). PLOS ONE 9(10): e107989, Doi: 10.1371/journal.pone.0107989 PMID: 25285822

29. Munir, A, Shahzad, A, Khan, M. (2014). Forced Convective heat transfer in boundary layer flow of Sisko fluid over a nonlinear stretching sheet. (2014) PLOS ONE 9(6): e100056,

30. Doi: 10.1371/journal.pone.0100056 PMID: 24949738

Table 2 Parameters and their descriptions

Parameter	Description	Parameter	Description
u,v	Velocity components along x and y axes	q_w	Heat transfer
D_B	Brownian diffusion coefficient	j_w	surface mass flux
D_T	thermophoresis diffusion coefficient	s	stretching rate
F	Non dimensional velocity	T	Temperature
$R_{ea,}R_b$	Local Reynold numbers	C	mass concentration
Nu_x	Nusselt number	$\propto$	thermal diffusivity
Sh_x	Sherwood number	θ	dimensionless temperature
L_e	Lewis number	φ	dimensionless concentration
P	Prandtl number	U	stretching velocity
B	Brownian motion	γ	chemical reaction parameter
T_p	Thermophoresis parameter	η	dimensionless variable
A	Sisko fluid parameter	ρ	fluid density

B_{i1}	Thermal Biot number	C_p	specific heat capacity of nano particles
C_{fx}	Local skin friction	κ	thermal conductivity
M	Magnetic field	υ	kinematic viscosity
R	radiation parameter	r	power law index
B_0	induced magnetic field	x,y	Coordinates
T_∞	Ambient temperature	C_w	concentration at the wall
T_w	uniform wall temperature	C_∞	ambient concentration
k_1	Chemical reaction coefficient	τ	Ratio of nanoparticle to base fluid